CREEP RESISTANCE AND MICROSTRUCTURE EVOLUTION IN SIMILAR WELD JOINTS MADE OF HR3C STEEL

Jakub ŘEHOŘEK [1, 3], Vlastimil VODÁREK [1], Zdeněk KUBOŇ [2]

[1]*VSB - Technical University of Ostrava, Ostrava, Czech Republic, EU, vlastimil.vodarek@vsb.cz*

[2] *Material and Metallurgical Research, Ltd, Ostrava, Czech Republic, EU, creep.lab@mmvyzkum.cz*

[3] *Research Centre Rez, Ltd, Pilsen, Czech Republic, EU, jakub.rehorek@cvrez.cz*

Abstract

Modern blocks of fossil fuel power plants designed for steam temperatures above 600 °C require advanced stainless steels in superheater or reheater systems. Great attention is paid to the exploitation of new steel grades with higher material properties. In the area of austenitic steels, the perspective grade is undoubtedly HR3C steel (X6CrNiNbN 25-20). In terms of the use of similar weld joints made of HR3C steel in fossil fuel power plants, detailed knowledge on creep resistance and microstructural stability of these weld joints is necessary.

Similar weld joints made of HR3C steel tubes were manufactured using a combination of GTAW and SMAW welding technologies. Weld joints were studied in both the as-welded state (PW), and after post-weld heat treatment (PWHT) at 1230 °C for 15 minutes. The paper presents the results of creep rupture tests on cross-weld samples tested at 650 and 700 °C. Metallographic analysis was performed on longitudinal sections of creep ruptured samples and microhardness HV 0.5 profiles over cross-weld samples were determined. The paper analyses the preferential rupture locations of the HR3C similar weld joints in dependence on the temperature of creep exposure and applied stress.

Keywords: HR3C steel, similar weld joints, PWHT, creep resistance, cross-weld samples.

1. INTRODUCTION

The new grades of austenitic stainless steels HR3C, Super304H and TP347HFG, along with higher creep strengths, also exhibit increased resistance to high temperature oxidation than previous generations of austenitic steels [1]. They were developed from AISI310S, AISI304H and AISI347H steels [1, 2]. Due to their balanced chemical composition, these are fully austenitic steels, in some cases with a low fraction of δ-ferrite [3]. This generation of materials is deployed in fossil power plants in superheaters and reheaters as well as previous generations [1]. The main alloying elements are chromium and nickel. Chromium stabilize ferrite, also provides corrosion resistance from a minimum level of 13 wt. % [4, 5]. The maximum chromium content is not more than 25 wt. % [6]. Higher chromium contents accelerate the formation of coarse particles of intermetallic σ-phase (Fe-Cr). Over 22 wt. % Cr has not been shown to affect positively the surface oxide layer [3]. Nickel, manganese and nitrogen stabilize austenite [4]. Nitrogen, except for austenite stabilization, increases Rp0.2 value. Low level of Rp0.2 is well known for austenitic steels [5]. According to [7], higher levels of Rp0.2 can also be achieved by additions of molybdenum and tungsten in austenitic steels [8]. A very important mechanism for increasing Rp0.2 is the precipitation of the thermodynamically stable intragranular phase. Precipitates must effectively hinder mobility of dislocations. Such a phase in austenitic steels is a N-rich Z-phase [9]. For Super304H steel, 3 wt. % Cu was added, niobium and nitrogen increased. ε-Cu particles in the austenitic matrix grow as spherical precipitates, which can affect the distribution of σ-phase [6]. This allows increases the corrosion resistance and creep properties of this steel grade. The chemical constitution of the TP347HFG steel has not been changed compared to the previous generation. HR3C steel has a defined nitrogen content compared to the previous steel generation (AISI310S). Higher nitrogen content reduces the susceptibility of this steel to undesirable σ-phase formation. Furthermore, HR3C steel has been alloyed by

niobium and nitrogen. The fine grain structure of HR3C, Super304H and TP347HFG steels is supported by the stabilization effect of niobium. It is advantageous for the homogeneous growth of the oxide layer on the inside surface of the superheater tubes. Fine grains allow easier transport of chromium to the surface, which is depleted. Easy continuous chromium transport to the surface allows the formation of a continuous homogeneous oxide layer. For HR3C steel, based on 25Cr-20Ni, growth of austenitic grains is effectively prevented by increasing the nitrogen content. TP347HGF and Super304H steels, based on 18Cr-8Ni, achieve fine austenitic grains by a combination of low-temperature forming and heat treatment [3]. The Super304H steel was in many cases processed with the shot peening technology (SP) [10].

The problem with characterization of real HR3C welds lies in the extremely narrow heat-affected zone (HAZ) [5, 7]. From this point of view, HAZ simulations can be very beneficial [5]. Therefore, it is necessary to carry out the complex check of the properties like creep resistance and microstructure evolution for both the base material and the weld joints [8, 11]. This paper deals with the influence of welding on HR3C material. The experimental similar welds were studied in both as-welded (PW) and post-weld heat treatment (PWHT) state. The preferential rupture locations of cross-weld samples were studied in dependence on the temperature of creep exposure and applied stress.

2. EXPERIMENTAL PROCEDURES

The evaluation of creep properties was carried out on cross-weld samples prepared from similar welds made of HR3C tubes with dimensions of ø38 x 6.3 mm. Weld joints were manufactured using automated orbital welding technology 141 (TIG, GTAW). Filler metal was a nickel-based alloy UTP A6170 Co (equivalent Thermanit 617). Cross-weld samples were cut from the similar welds in the as-welded state (PW) and also after post-weld heat treatment (PWHT) and were carried out at 1230 °C in 15 min in the water. Chemical composition of the steel investigated is shown in **Table 1**.

Table 1 Chemical composition of the HR3C steel, wt. %

C	Mn	Si	P	Cr	Ni	N	Nb
0.06	1.19	0.41	0.016	24.9	19.9	0.26	0.44

Mechanical properties of HR3C steel tubes in the as-received state (AR), are summarised in **Table 2,** where *RA* represent creep rupture ductility. Long-term creep rupture tests with a constant tensile load were carried out in air at temperatures of 650 and 700 °C. The stress dependences of the time to rupture were described by the Seifert parametric equation (1) [12]:

$$\log(\sigma) = A_1 + A_2 \cdot P + A_3 \cdot P^2 \;\; ; \;\; P = T \cdot [\log(t_r) + A_4] \cdot 10^{-4} \qquad (1).$$

where σ is the initial applied stress, T is the test temperature, t_r is the time to rupture, A_1 to A_4 are constants and P is parameter. The equation (1) was applied for the calculation of the $R_{m/650°C/10^5h}$ and $R_{m/700°C/10^5h}$ values. The creep properties of the cross-weld samples made of similar HR3C welds are compared in **Figures 1**(a) and **1**(b) with the creep characteristics of the base HR3C material a reference [2].

Table 2 Mechanical properties of HR3C tubes tested in the AR state

$R_{p0.2}$ (MPa)	R_{p1} (MPa)	R_m (MPa)	RA (%)
186	362	748	46

Creep tests to rupture and microstructural investigations were conducted on cross-weld samples in two states: as-welded (PW) and after post-weld heat treatment (PWHT) and were investigated in order to understand the processes responsible for failure mechanism and creep behaviour. Creep parameters and rupture location are for experimental specimens summarized in **Table 3**. Investigations were carried out by means of optical

microscopy (LOM) and scanning electron microscopy (SEM) on longitudinal sections of creep ruptured samples. Longitudinal sections were prepared by electrical discharge machining. Microstructure for LOM investigations was revealed by etching in a V2A etchant. Coarsening of austenitic grains in HAZ was studied using SEM-EBSD after electrolytic polishing of samples. The size and distribution of austenitic grains in selected parts of welds were determined. Finally, microhardness HV 0.5 profiles on longitudinal sections of cross-weld specimens were evaluated.

Table 3 Creep parameters and rupture locations of cross-weld specimens investigated

Specimen	State of weld	Temperature (°C)	Stress (MPa)	Time to Rupture (h)	RA (%)	Rupture Location
A1	PW	650	160	8968	51.1	BM
A2	PW	650	120	22256	5.6	HAZ
A3	PW	650	110	37672	1.6	HAZ
B1	PW	700	75	16883	-	HAZ
C1	PWHT	700	140	1188	14.7	WM
C2	PWHT	700	100	6958	-	HAZ
C3	PWHT	700	90	15712	-	HAZ
C4	PWHT	700	75	14531	13.4	BM

3. RESULTS

Results of long-term creep rupture tests at 650 and 700 °C are shown in **Figures 1**(a) and **1**(b), respectively. Specimens selected for microstructural characterization are marked A1 to A3, B1 and C1 to C4. The red marks indicate specimens just before rupture.

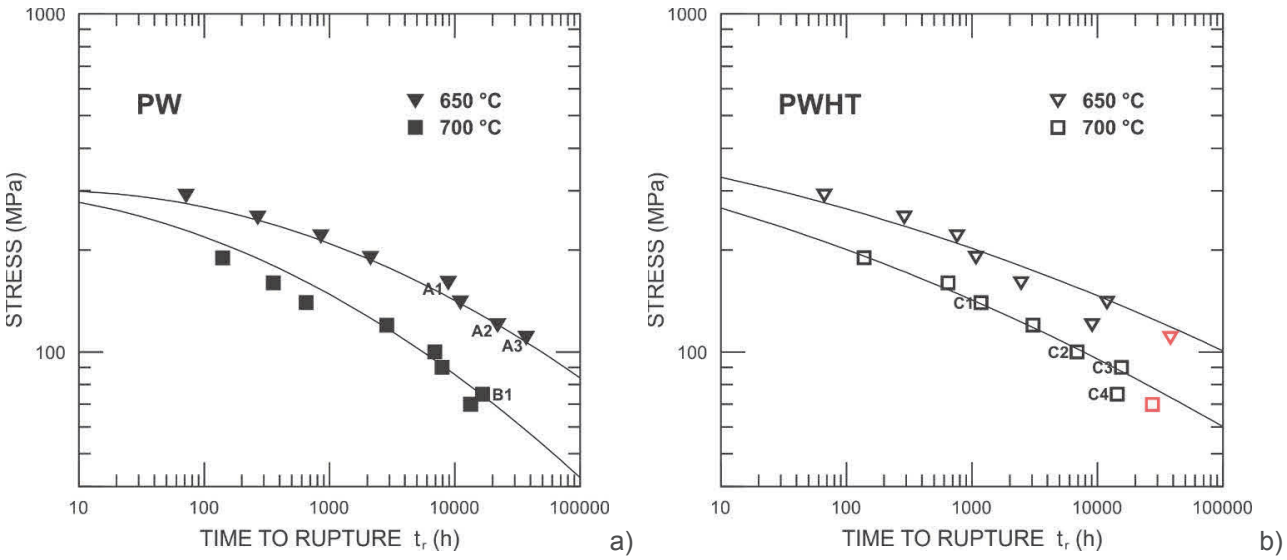

Figure 1 Dependence of stress on time to rupture, (a) as-welded (PW) state, (b) post-weld heat treatment (PWHT) state

The results of creep strength calculations for 10^5 hours at temperatures of 650 and 700 °C are shown in **Table 4**. The standardized creep strength values of the HR3C steel at 650 and 700 °C after 10^5 hours are 114 and 66 MPa, respectively [2], which means that the long-term creep strength of the tested material is in the allowable limit ±20 % around the mean standardized value. What is very interesting is the fact that both the

base material and the weld joint tested after PWHT have at both temperatures practically the same calculated $R_{m/T/10^5h}$ values, **Table 4**.

Table 4 Calculated long-term creep strength values (MPa) for 10^5 hours at 650 and 700 °C, according to (1) for base material (BM) and cross-weld (CW) samples

Location	PW		PWHT	
	650 °C	700 °C	650 °C	700 °C
BM	102	58	102	60
CW	84	43	101	60

Creep rupture ductility (RA) values showed a pronounced decline with prolonging time to rupture at both temperatures investigated, **Table 3**

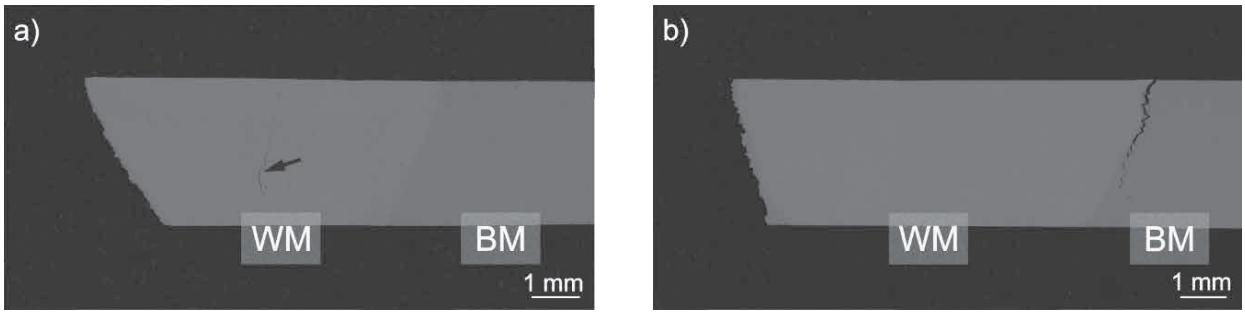

Figure 2 Fracture line profiles in the HAZ, longitudinal sections, BSE images a) Specimen A3, PW state, b) Specimen C3, PWHT state

Figures 2(a) and **2**(b) show rupture locations in cross-weld specimens A3 and C3, respectively. In both samples failure occurred in the HAZ. In the sample A3 creep damage is also present in the weld metal - see the arrow in **Figure 2**(a). Creep damage in the sample C3 is present in the HAZ on both sides of the WM. It proved that creep damage could simultaneously develop in several parts of the cross-weld samples and the final failure occurred in the weakest location.

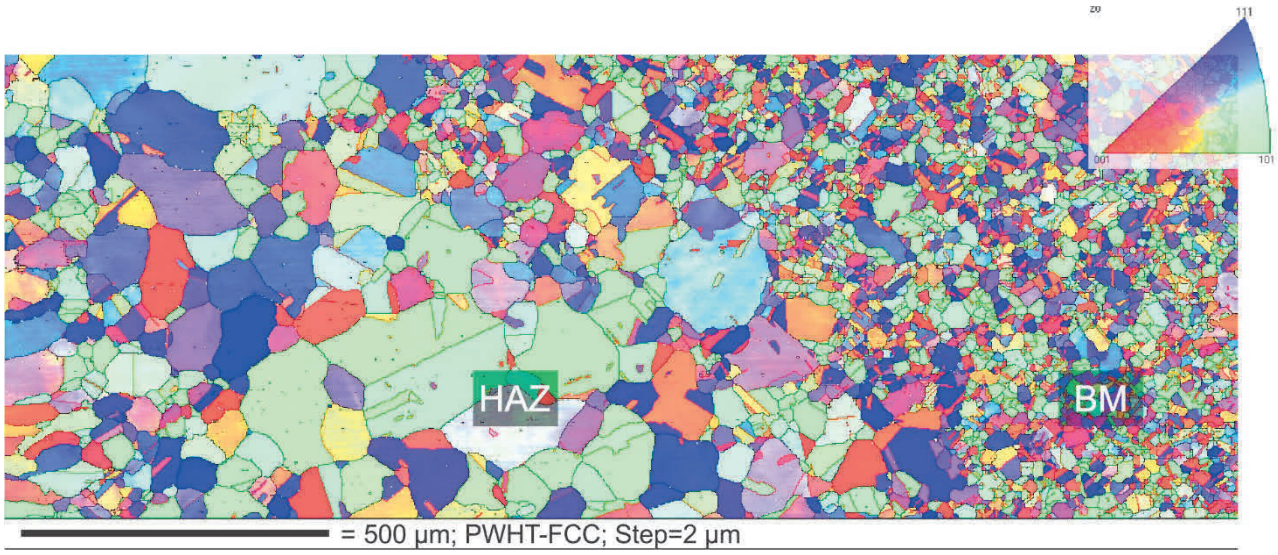

Figure 3 IPF orientation map for ND direction showing coarsening of austenitic grains in the heat-affected zone of the weld, longitudinal section, Specimen A1

Table 3 summarises rupture locations. Creep rupture in most cross-weld samples investigated occurred in the HAZ. In some cases cross-weld samples failed either in the BM or in the WM. **Figure 3** shows crystal orientation map for the specimen A1 in an area of the HAZ and the adjacent BM. Colour legend of the inverse pole is in **Figure 3** in the top right corner. The average austenite grain size close to the fusion zone was 85 μm, at the distance of 500 μm from the fusion zone it was 30 μm, and in the base material the average austenite grain size was about 7 μm.

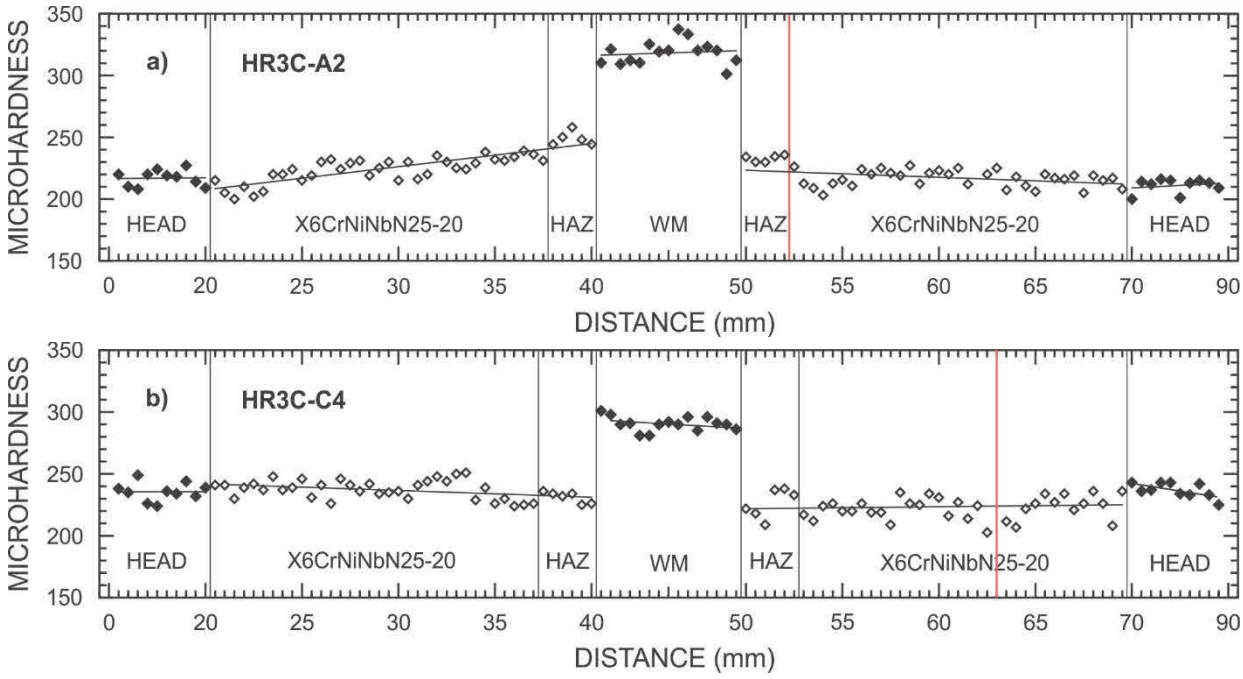

Figure 4 Microhardness HV 0.5 profile along longitudinal sections of creep ruptured specimens, a) Specimen A2, b) Specimen C4

Microhardness can reflect the evolution of microstructure in materials. Microhardness was measured according to ASTM E384. Microhardness HV 0.5 profiles in the A2 and C4 specimens are shown in **Figures 4**(a) and **4**(b), respectively. Microhardness of the BM in the specimen A2 has on both sides a rising tendency from the head towards the weld metal. In the Specimen C2 a slight decline of microhardness from the head toward the weld metal was observed. The rupture location is indicated by a red line.

4. DISCUSION

The curves in **Figure 1** and results of creep rupture tests on cross-weld samples prove that creep properties of the HR3C similar weld after PWHT at 1230 °C are for both temperatures investigated better than those for the weld in the as-welded state. Performed creep rupture tests on cross-weld and base material of HR3C steel revealed that the extrapolated long-term creep strength of the weld joint was very close to that of the base material. Such behaviour was detected in austenitic creep resistant steel before in cases when overmatching (having higher mechanical and/or creep strength) weld metal was used. In these cases, the critical failure location moved in higher temperatures and longer times from HAZ into BM and weld joint did not longer represent the weakest part of structure [13].

Metallographic investigations on creep ruptured specimens in the as-welded state revealed a narrow HAZ defined by coarsened austenitic grains. One-step PHWT at 1230 °C resulted in more pronounced coarsening of austenitic grains in the HAZ. Coarse-grained structure is typically more prone to intergranular corrosion. Intergranular corrosion can significantly reduce the life of the material.

5. CONCLUSION

Creep rupture tests on cross-weld samples of the HR3C similar weld revealed that the long-term creep strength of the weld joint was in the allowable limit ±20 % around the standardized value and the extrapolation of experimental results confirmed that with increasing temperature and time to rupture the both base material and weld joints have practically the same creep rupture strength. Creep rupture results obtained on cross-weld samples in the state after post-weld heat treatment at 1230 °C for 15 minutes were better than those obtained on cross-weld samples in the as-welded state.

Metallographic analysis revealed coarsening of austenitic grains in the HAZ due to thermal cycle during welding. Coarsening of austenitic grains in the HAZ was more pronounced in samples after the post-weld heat treatment at 1230 °C. Creep failure in most cross-weld samples investigated occurred in the HAZ. Creep damage usually developed in several areas of cross-weld samples and the final failure occurred in the weakest location.

ACKNOWLEDGEMENTS

The presented work was financially supported by the Ministry of Education, Youth and Sport Czech Republic - project LQ1603 Research for SUSEN. This work has been realized within the SUSEN Project established in the framework of the European Regional Development Fund (ERDF) in project CZ.1.05/2.1.00/03.0108 and of the European Strategy Forum on Research Infrastructures (ESFRI) in the project CZ.02.1.01/0.0/0.0/15_008/0000293, which is financially supported by the Ministry of Education, Youth and Sports - project LM2015093 Infrastructure SUSEN.

REFERENCES

[1] EPRI RESEARCH INSTITUTE. *Boiler Materials for USC Plant* [online]. Created on 2003. 28 p. [viewed 2018-02-26]. Available from: https://netl.doe.gov/File%20Library/Events/2003/materials/Viswanathan.pdf

[2] VdTÜV MATERIAL SHEET. *Heat Resistant Rolling and Forged Steel X6CrNiNbN25-20 (1.4952)*. 2009. 5 p.

[3] YOSHIKAWA, K., TERANISHI, H., TOKIMASA, K. Fabrication and Properties of Corrosion Resistant TP347H Stainless Steel. *Journal of Materials Engineering*, 1988, vol. 10, no. 1, pp. 69-83.

[4] LO, K.H., SHEK, C.H., LAI., J.K.L. Recent developments in stainless steels. *Materials Science and Engineering*, 2009, vol. 65, no. 4, pp. 39-104.

[5] ZOHU, Y., LIU, Y., ZOHU, X. Precipitation and hot deformation behavior of austenitic heat-resistant steels. *Journal of Materials Science & Technology*, 2017, vol. 33, no. 12, pp. 1448-1456.

[6] ROSSER, J.C., BASS. M.I., COOPER C., Steam oxidation of Super 304H and shot-peened Super 304H. *Materials at High Temperatures*, 2014, vol. 29, no. 2, pp. 95-106.

[7] SKLENIČKA, V., KUCHAŘOVÁ, K., KVAPILOVÁ, M. Creep properties of simulated heat-affected zone of HR3C austenitic steel. *Materials Characterization*, 2017, vol. 128, pp. 238-247.

[8] ZHANG Z., HU. Z., TU, H. Microstructure evolution in HR3C austenitic steel during long-term creep at 650 °C. *Materials Science and Engineering*, 2016, vol. 681, pp. 74-84.

[9] VODÁREK, V. Stability of Z-phase and M6X in creep-resistant steels. *Scripta Materialia,* 2012, vol. 66, no. 9, pp. 678-681.

[10] NARULA R.G., KOZA, D., WEN, H. Impacts of steam conditions on plant materials and operation in ultra-supercritical coal power plants. *Ultra-Supercritical Coal Power Plants*, 2013, pp. 23-56.

[11] WANG, B., LIU, Z., CHENG, S. Microstructure Evolution and Mechanical Propertiesof HR3C Steelduring Long term Agingat High Temperature. *Journal of Iron and Steel Research*. 2014, vol. 21, no. 8, pp. 765-773.

[12] SEIFERT, W. *Heat-resistant Metallic Materials*, Technical Institute, Zittau, 1977.

[13] ASME MATERIAL STANDARD. *Boiler and Pressure Vessel Code, Code Case N-47-32: Class 1 Components in Elevated Temperature Service.* 1998.